Proceedings of the ASME 2021
Pressure Vessels & Piping Conference
PVP2021
July 12-16, 2021, Virtual, Online

PVP2021-62878

PREDICTION OF J-INTEGRALS AT DEFECTS IN W-9CR STEEL SANDWICH-TYPE COOLING PIPES

Tristan Calvet
Dept. of Mechanical Engineering, Imperial College London, SW7 2BU, UK
t.calvet19@imperial.ac.uk

Yiqiang Wang
Culham Centre for Fusion Energy,
UK Atomic Energy Authority
Abington, OX13 3DB, UK
yiqiang.wang@ukaea.uk

Minh-Son Pham
Dept. of Materials, Imperial College London, SW7 2BU, UK
son.pham@imperial.ac.uk

Catrin M. Davies
Dept. of Mechanical Engineering, Imperial College London, SW7 2BU, UK
catrin.davies@imperial.ac.uk

ABSTRACT

Sandwich-type cooling pipes of the first wall of future fusion nuclear reactors (i.e. DEMO) will likely consist of tungsten brazed to a Reduced Activation Ferritic Martensitic (RAFM) steel. Under a high heat flux (HHF) (1-5 MW/m^2) the mismatch in thermal expansion between tungsten and steel results in significant thermal stresses in the brazing region. These stresses can cause crack initiation and growth and thus compromise the structural integrity of such pipes. Finite element analyses have been performed on the brazed joints of a reference cooling assembly under HHF. Thermal stresses and resulting plastic strains were estimated for both the braze interlayer and parent materials. As images of brazed joints revealed, brazing processes are very likely to induce defects near the edges of the joints. A crack is therefore introduced in the brazed region where simulated stresses and strains are found to be the highest. J-integrals were calculated for cracks growing from an edge to the center of the considered piping assembly. The results are discussed in relation to the current sandwich-type piping design of the DEMO reactor.

Keywords: DEMO, First Wall, High Heat Flux, Brazing, Thermal Stresses, Defects, J-integrals.

NOMENCLATURE

Abbreviations:

DEMO	European DEMOnstration fusion power plant
FW	First Wall
HHF	High Heat Flux
HIP	Hot Isostatic Pressure
PFC	Plasma Facing Component
RAFM	Reduced Activation Ferritic Martensitic

Symbols:

α	Linear coefficient of thermal expansion (K^{-1})
Δ	Variable distance (m)
ε_p	Plastic Strain (-)
ε_u	Uniform elongation (-)
λ	Thermal conductivity (Wm^{-1}K^{-1})
σ_u	Ultimate true tensile strength (Pa)
σ_y	Tensile true yield strength (Pa)
τ	Tangent modulus (Pa)
ν	Poisson ratio (-)
φ	Heat Flux (Wm^{-2})
a	Crack length (m)
E	Young's modulus (Pa)
h	Heat transfer coefficient (Wm^{-2}K^{-1})
K	Strength coefficient (-)
n	Strain hardening exponent (-)
T_m	Liquidus temperature (K)

1. INTRODUCTION

To extract the heat from HHF in the DEMO fusion reactor, several baseline first wall cooling concepts, based on helium or water cooling have been developed [1], [2]. The concepts principally rely on Eurofer97, a Reduced Activation Ferritic

Martensitic (RAFM) steel, being used as structural material, and tungsten used as a refractory plasma facing material. Such designs of the cooling assemblies have been reported to have heat flux limits of around 1 to 1.5 MW/m^2.

During reactor operation, under HHF, the cooling assemblies will be subject to significant thermal stresses resulting from the large difference in thermal expansion of tungsten and Eurofer97. Additionally, DEMO operation will seemingly consist in thousands of loading pulses lasting up to a few hours [3]. In this respect, cooling assemblies and especially tungsten-Eurofer97 joints will be exposed to both fatigue and creep processes, which will further affect the structural integrity of the First Wall (FW).

Brazing is considered to be a promising technique in joining tungsten to Eurofer97. Although no definitive brazing alloy is yet selected, Cu-based alloys with high ductility and high temperature fracture strength are promising alloys since they may mitigate thermal stresses by extensive plastic deformation. However, only few structural integrity analyses take into consideration the brazing interlayer that separates the tungsten armor tiles and the cooling channels and more importantly, the residual stresses and defects resulting from the brazing of materials.

In this study, firstly, the resulting stresses and strains from steady-state HHF have been estimated in a reference single cooling channel (FIGURE 1 and FIGURE 2). Subsequently, a defect of the form of a sharp crack has been introduced at the edge of the braze joint. J-integrals are calculated and the influence of both heat flux intensity and crack length on the J-integrals are estimated. Results are then compared with estimations of initiation fracture toughness from the literature [4] for copper alloys at high temperatures (350+°C). Some discussion is then presented on the role of the brazing alloy and its thickness to minimize values of J-integrals at defects under high heat fluxes.

2. MATERIALS AND METHODS

2.1 Geometry and Mesh Details

A sandwich-type cooling assembly with rectangular cooling channel was chosen as the reference design for this study (FIGURE 1). Most of the dimensions of this reference cooling channel design, although yet definitive, were obtained from [5]. The whole cooling assembly cross section is 72 mm in width and is 21 mm in height, and consists of four 18 mm wide cooling channels. A full cooling assembly is usually about one meter in length. The Eurofer thickness separating tungsten to the coolant is 3 mm and the tungsten tile thickness is 2 mm. A typical braze thickness of 100 µm was chosen as reference.

A 2D plain strain model was built from these dimensions (FIGURE 2) under the simulation software ABAQUS [6]. Given the significant dominance of stresses at the brazing interface, and the brushed design of the cooling channels with tungsten tiles, only a single channel is modelled.

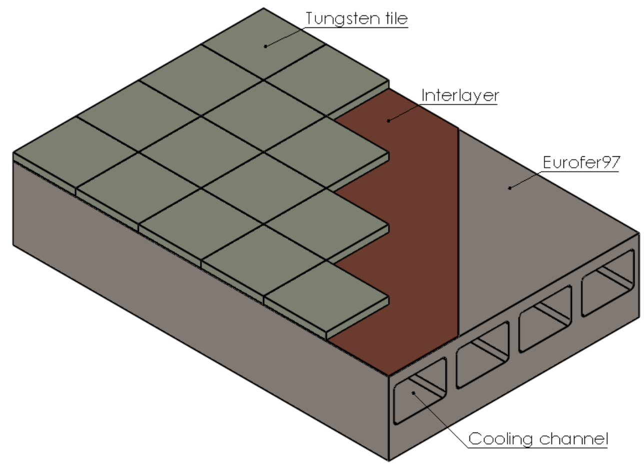

FIGURE 1: 3D SECTION OF A FIRST WALL COOLING ASSEMBLY **[5]**.

In the heat transfer analyses, the mesh consisted of 13,000 4-node linear heat transfer quadrilateral 2-D elements (DC2D4). For the mechanical analyses, 24,472 2-D continuum 4 nodded reduced integration point elements (CPE4R) were used (FIGURE 3). In the braze-interlayer, the elements were 10 µm in size.

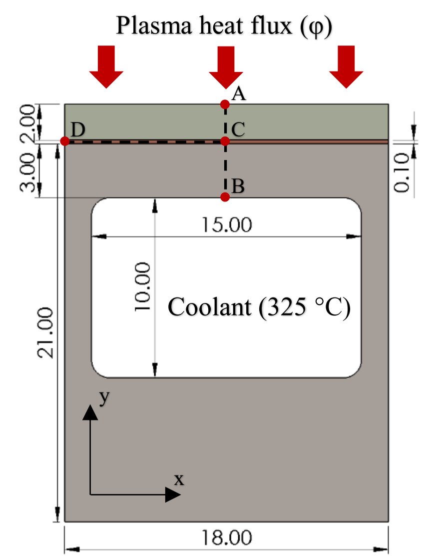

FIGURE 2: DIMENSIONS IN mm OF A SINGLE COOLING CHANNEL **[5]**.

In the second part of the study, a sharp crack parallel to the interlayer was introduced at its edge, growing towards the center of the assembly. The crack seam was considered as a perfect insulator in the thermal analysis. At the crack-tip, J-integrals were obtained from averaging 10 contour integrals calculated using fine element sizes ranging from 1 µm to 10 µm and a maximum outer contour diameter of 80 µm.

The thermal stresses were obtained by first calculating nodal temperature from steady state thermal analyses under varying HHF from 0.5 to 2 $MW.m^{-2}$ (FIGURE 4 and FIGURE 5). The incoming heat flux is applied uniformly on the top surface of the tungsten tile. In analyses, the coolant temperature was taken to be 325 °C and the fluid-solid heat transfer coefficient (h) was chosen as equal to 60 $kW.m^{-2}.K^{-1}$, which is representative of moderate cooling capacities of FW cooling assemblies. The convective heat transfer occurs between the coolant and the inner surface of the channel. For all the other external surfaces of the channel, adiabatic boundary conditions were assumed. In simulations involving J-integrals, the crack seam was considered as a perfect insulator.

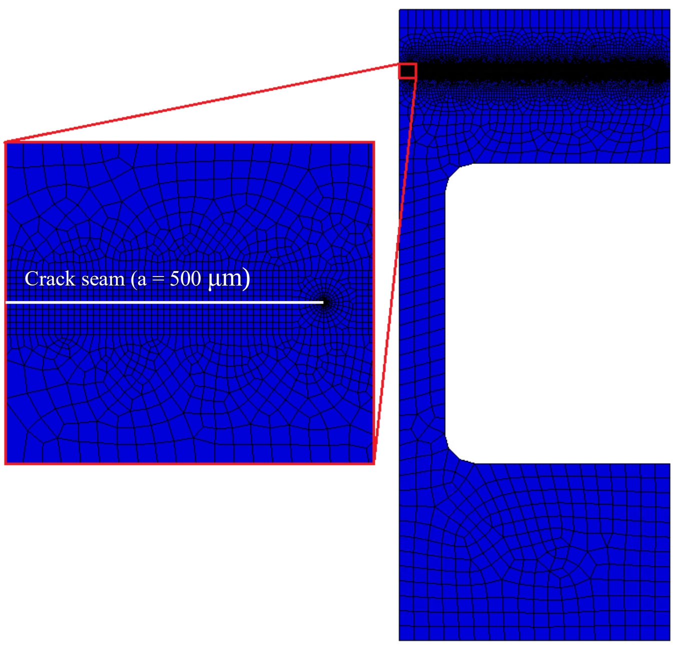

FIGURE 3: 2D MESH FOR THE LEFT-HALF OF THE COOLING CHANNEL AND AROUND THE CRACK SEAM (a = 500 µm).

In the stress analysis, the resulting temperature field was mapped onto the cooling channel to determine the resulting thermal stresses, equivalent plastic strains and J-integrals. The initial temperature of the assembly at the stress of the stress analysis was assumed uniform and equal to 22°C. During the analysis, solely a boundary condition preventing rotation was used on both of the steel side edges of the channel.

2.2 Material Properties

The coefficients of thermal expansions (α), thermal conductivity of all materials (λ) and liquidus temperatures (T_m) are given in TABLE 1 and **TABLE** 2.

TABLE 1: LIQUIDUS TEMPERATURES OF MATERIALS.

Material	Tungsten	Copper	Eurofer97
T_m (K)	3700	1350	1750

TABLE 2: LINEAR COEFFICIENT OF THERMAL EXPANSION AND THERMAL CONDUCTIVITIES FOR EUROFER97, COPPER AND TUNGSTEN ([7], [11], [12], [13]). (NOTE: COEFFICIENT OF THERMAL EXPANSION OF F82H USED INSTEAD AS DATA YET TO BE AVAILABLE FOR E97).

Temp.		Eurofer97 ([7])		Copper ([11], [13])		Tungsten ([13], [14], [12])	
T (K)	T (°C)	$\alpha\times10^{-6}$ (K^{-1})	λ ($Wm^{-1}K^{-1}$)	$\alpha\times10^{-6}$ (K^{-1})	λ ($Wm^{-1}K^{-1}$)	$\alpha\times10^{-6}$ (K^{-1})	λ ($Wm^{-1}K^{-1}$)
293	20	-	28.34	16.4	386	4.3	170
373	100	10.7	29.2	17.4	384	4.5	159
473	200	11	30.67	18.0	380	4.6	146
573	300	11.2	30.2	18.6	375	4.7	137
673	400	11.7	29.33	19.3	370	4.8	130
773	500	12	29.45	20.0	364	-	125
873	600	12.3	31.17	-	358	-	122
1500	1227	-	-	-	-	5.43	107
2000	1727	-	-	-	-	6.25	100

Due to the limited available experimental data at high-temperature, different models were used to describe the mechanical properties of tungsten, copper and Eurofer97. A Ramberg-Osgood material model (Equations 1-3) was used to describe the tensile behavior of Eurofer97 for which sufficient experimental data was recovered from [7]:

$$\varepsilon = \frac{\sigma}{E} + K\left(\frac{\sigma}{\sigma_y}\right)^n \tag{1}$$

where σ_y is the yield stress, n is the strain hardening exponent and K is the yield offset parameter:

$$K = \varepsilon_{0.2} - \frac{\sigma_y}{E} \tag{2}$$

$$n = \frac{\ln\left(\varepsilon_u - \frac{\sigma_u}{E}\right) - \ln(K)}{\ln(\sigma_u) - \ln(\sigma_y)} \tag{3}$$

Although, herein, K is taken as constant (K=0.002).

Given limited high-temperature experimental data in the literature, the properties of tungsten were described using a simple elastic-plastic bilinear model:

$$\sigma = \sigma_y + \tau\left(\varepsilon - \frac{\sigma_y}{E}\right) \tag{4}$$

where τ is the material tangent modulus.

Copper properties covering a wide range of temperatures were obtained from [8] and derived from a Johnson-Cook model (Equations 5 and 6) [9]:

$$\sigma_y = \left[A + B\left(\varepsilon_p\right)^n\right]\left(1 - (T^*)^m\right) \tag{5}$$

where:

$$T^* = \frac{T - T_0}{T - T_m} \tag{6}$$

where T_0 is the reference temperature ($T_0 = 293$ K).
The chosen properties based on the described model applied to materials are given in TABLE 3, TABLE 4 and TABLE 5.

TABLE 3: MECHANICAL PROPERTIES OF TUNGSTEN [15].

T (K)	T (°C)	ν (-)	E (GPa)	σ_y (MPa)	τ (GPa)
293	20	0.28	398	1360	1.3
473	200	-	397	1154	1.2
673	400	-	394	947	1.1
873	600	-	389	764	1.0
1073	800	0.29	379	604	0.9
1273	1000	-	368	465	0.8
1773	1500	0.3	333	204	-
2073	1800	-	306	103	-

TABLE 4: MECHANICAL PROPERTIES OF EUROFER97 **[7]**. (*NOTE: YOUNG MODULUS OF F82H USED INSTEAD AS DATA YET TO BE AVAILABLE FOR E97).

T (K)	T (°C)	ν (-)	E (GPa)*	σ_y (MPa)	σ_u (MPa)	ε_u (-)
293	20	0.29	217	546	668	0.052
373	100	-	212	507	622	0.050
473	200	-	207	484	581	0.041
573	300	-	203	470	545	0.031
673	400	-	197	447	499	0.021
773	500	-	189	396	428	0.014
873	600	-	178	298	316	0.012
973	700	-	161	135	148	0.018

TABLE 5: COPPER JOHNSON-COOK MODEL PARAMETERS **[8]** AND POISSON RATIO.

Material	A (MPa)	B (MPa)	n (-)	m (-)	ν (-)
Copper	99.7	262.8	0.23	0.98	0.34

3. RESULTS AND DISCUSSION

3.1 Stress analysis of the defect free channel

Results from the thermal analysis (FIGURE 4) suggest that about 1.5 MW.m^{-2} is the maximum allowable steady state HHF of the cooling assembly due to the 550°C temperature threshold of Eurofer97 [7]. Beyond this threshold, the creep properties of Eurofer97 are known to degrade consequently, thus compromising the integrity of the assembly.

Temperatures fields and resulting σ_{xx} stress fields are depicted in FIGURE 5 and FIGURE 6. The most significant stresses resulting from the thermal expansion mismatch of tungsten and Eurofer97 were found at the interface where tungsten and Eurofer97 respectively constrain each other's thermal expansion. This results in principally tensile stresses in tungsten and compressive stresses in Eurofer97 along the x-direction (σ_{xx}).

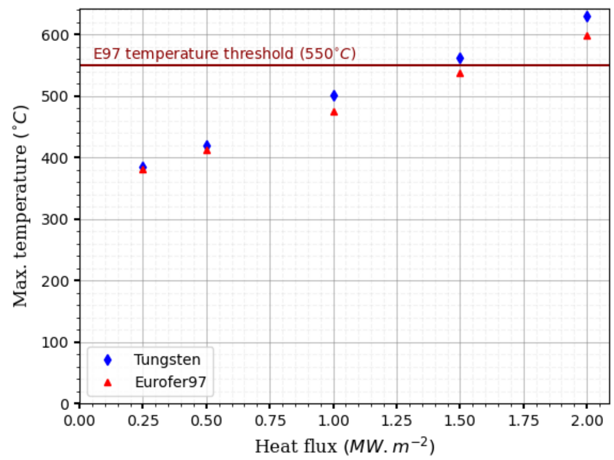

FIGURE 4: MAXIMUM TEMPERATURE IN BOTH EUROFER (E97) AND TUNGSTEN (W) VERSUS INCOMING HHF.

In FIGURE 6, stresses near the interlayer are found to decrease with higher heat fluxes. This is explained by the increase in temperature of the interlayer at higher HHF, allowing for larger plastic deformation of the copper interlayer and therefore mitigating further thermal stresses.

Inside the interlayer, maximal principal stresses of about 250 MPa and maxima strains of 5-10% were located close to the point D region (FIGURE 7, FIGURE 8). Considering the cyclic nature of the HHF and resulting thermal strains in the interlayer, fatigue cracks would most likely initiate from the edge of the interlayer. Potential defects resulting from the brazing process are similarly likely to appear in this same region due to the resulting brazing high plastic strains. The development of such defects is well observed in the literature notably at edges and corners of brazed tiles [10]. The edge of the interlayer was therefore chosen to introduce a sharp crack, as described in Section 3.2.

In addition to extensive plastic strains, a singularity at the interface between the interlayer and Eurofer97 is seen in FIGURE 7. Simulations suggests that it results from the discontinuous interface in combination with high tensile thermal stresses (σ_{yy} > 200 MPa) observed in Eurofer97 directly below point D. The strains and stresses at the singularity could further facilitate the initiation and growth of defects and cracks, giving supplementary evidence of the importance of the brazed tiles edges for the development of cracks.

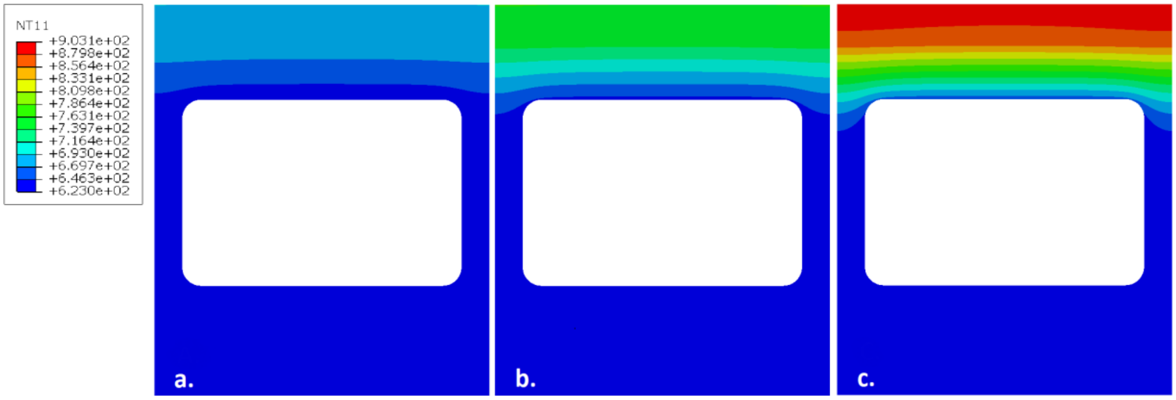

FIGURE 5: TEMPERATURE (K) FIELD FOR VARYING INCOMING HHF: a. 0.5 MW.m^{-2}, b. 1 MW.m^{-2}, c. 2 MW.m^{-2}.

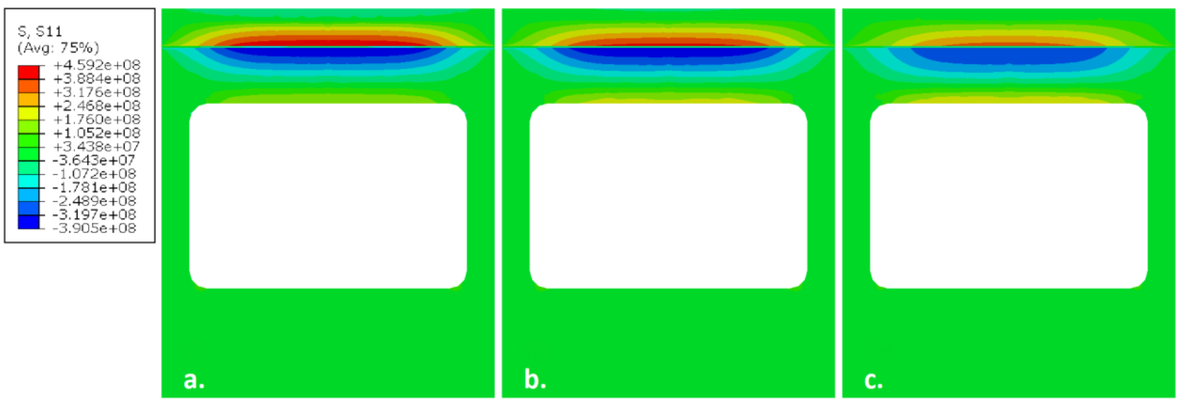

FIGURE 6: STRESS (σ_{xx}) FIELD FOR VARYING HHF: a. 0.5 MW.m^{-2}, b. 1 MW.m^{-2}, c. 2 MW.m^{-2}.

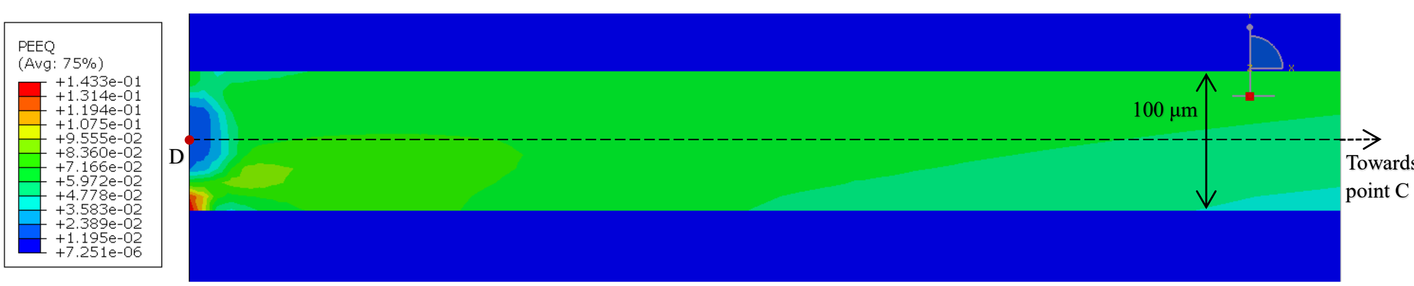

FIGURE 7: EQUIVALENT PLASTIC STRAIN FIELD IN 100 um BRAZED JOINT FOR INCOMING HHF OF 1 MW.m^{-2}.

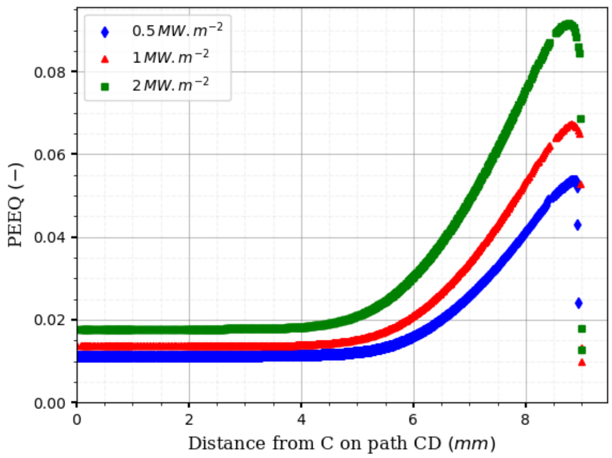

FIGURE 8: EQUIVALENT PLASTIC STRAIN FOR BRAZING ELEMENTS ALONG PATH CD FOR HHF OF 0.5, 1 AND 2 MW.m^{-2} (C at 0 mm and D at 9 mm).

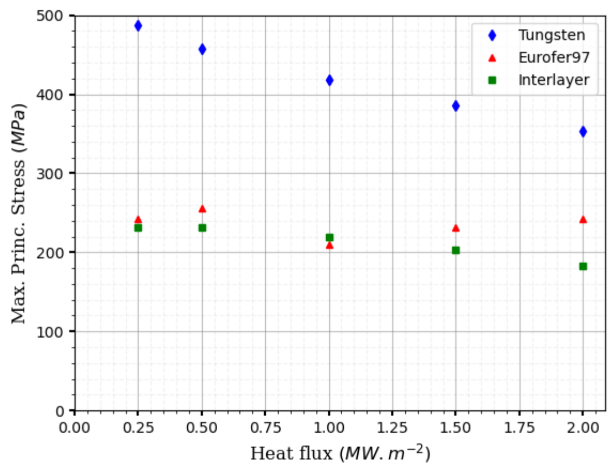

FIGURE 9: MAXIMUM PRINCIPAL STRESSES IN MATERIALS OF THE ASSEMBLY VERSUS INCOMING HHF (MW.m^{-2}).

To mitigate the impact of singularities, thermal stresses and plastic strains on the structural integrity of cooling channels, thicker, more ductile and less thermally expansive brazing alloys should be sought. This would potentially allow cooling assemblies to sustain high HHF for an increased number of cycles by limiting the growth of defects in the brazing-alloy. However, temperature fields would remain unchanged signifying any steady-state HHF greater than 1.5 MW.m^{-2} would remain unsuitable for the assemblies.

To improve HHF capabilities, the thickness of Eurofer97 separating the interlayer from the coolant would need be decreased. Although, lessening this thickness would allow for higher HHF capabilities, a low Eurofer97 thickness would favor plastic and creep strains, potentially displacing the failure risk from the brazing alloy to the more critical steel cooling channel. Preliminary simulations show the importance of the modification of the Eurofer97 thickness through important variations of the J-integrals values.

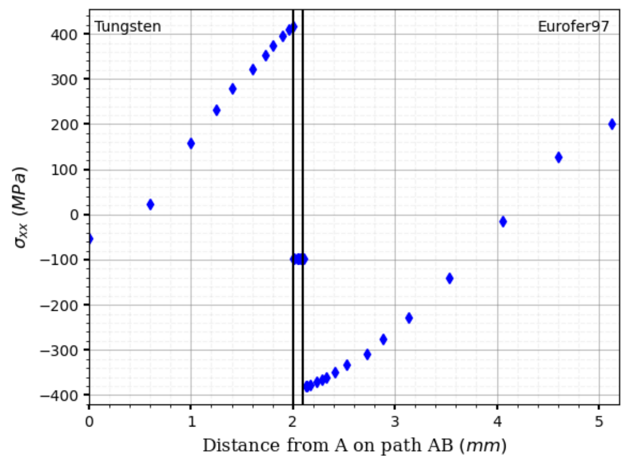

FIGURE 10: σ_{xx} ON PATH AB FOR AN INCOMING HHF OF 1 MW.m^{-2}. WHERE THE TOP OF THE TUNGSTEN TILE IS AT 0 mm AND THE EUROFER97-COOLANT INTERFACE IS AT 5.1 mm.

The maximum principal stresses found in the assembly for each metal were reported in FIGURE 9. They are shown to vary slightly for Eurofer97 and the interlayer but decrease significantly for tungsten with an increase of the incoming heat flux. The stress relaxation may result principally from the increase in temperature of the interlayer allowing for further plastic deformation. This stress variation of tungsten suggests it could be particularly impacted by the cyclic reactor pulses and potential transients. Related fatigue processes may cause defect growth and delamination at the tungsten brazing interface where σ_{xx} thermal stresses are the most significant in both tungsten and Eurofer97 (FIGURE 10). The introduction of a thicker interlayer needs also, in this regard, to be studied to estimate its potential impact on mitigating the thermal stress gradient seen across the joint and the related range of stress intensity in fatigue processes.

3.2 J-integrals of braze-joint defects

According to the stress state previously discussed, a horizontal sharp crack is introduced at the center of the brazed joint starting from point D (FIGURE 3). J-integrals are calculated for varying crack-lengths (FIGURE 11) or heat fluxes (FIGURE 12). Results obtained suggest a significant impact of both the incoming heat flux and the defect length on J-integrals. The greatest variation of J-integrals is seen when very short defects (10-20 µm) increase slightly in length. Once a crack length of around 500 µm is reached, a plateau of the J-integral is observed from simulations, indicating that crack length has limited influence on crack-growth after reaching a certain size. Due to the resulting stresses in the assembly from the thermal expansion mismatch of parallel brazed surfaces, stresses normal to the crack seam (σ_{yy}) remain very limited around the crack-tip. It suggests that the crack-tip deformation is driven principally by in-plane shear stresses (Mode II).

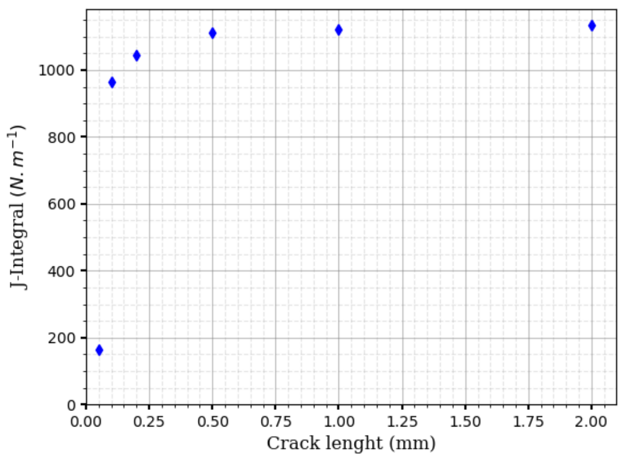

FIGURE 11: J-INTEGRAL (N.m^{-1}) VERSUS CRACK LENGTH (mm) FOR INCOMING HHF OF 1 MW.m^{-2}.

The initiation fracture toughness (J_{IC}) at temperatures up to 350 °C for two copper alloys (CuAl25, CuCrZr) have been reported in [4]. In this reference, J_{IC} was found to decrease significantly with an increase of temperature especially for CuAl25. At 350 °C, the CuAl25 initiation fracture toughness was inferior to 5000 N.m^{-1} but HIP joints created with CuAl25 had notably lower J_{IC}. In this regard, it is expected that J_{IC} may also be reduced in copper brazed joints.

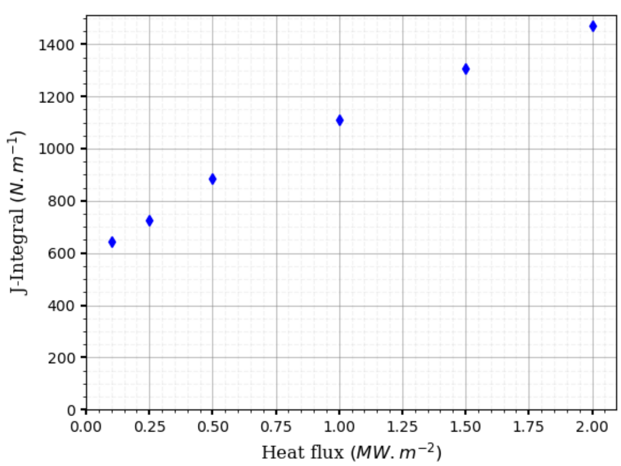

FIGURE 12: J-INTEGRAL (N.m^{-1}) VERSUS INCOMING HHF (MW.m^{-2}) FOR A 500 µm CRACK.

Under 1 MW.m^{-2}, temperatures of around 480 °C (FIGURE 4) are expected in the brazed joint, indicating that the brazed joint J_{IC} could be less than the estimated J-integral values from the from simulations (eg. 1100 N.m^{-1} for a = 500 µm). However, CuCrZr retain high J_{IC} [4] at 350 °C: 50 000 N. m^{-1} in HIP joints at 200 °C. It indicates some copper alloys suitable for brazing could retain a high initiation fracture toughness at high temperatures.

Predictions of J-integrals were also influenced by the model limitations. Assumptions of the 2D modelling such as the plain strain assumption, the considered isotropic properties, the shape of the defect and its position do affect obtained results in the conducted simulations. For instance, additional strains in the Z-direction for a 3D-model would increase the maximum strains seen in the interlayer, notably at the tile corners. Higher J-integrals may then be expected for defects developing at corners as shown experimentally in [10].

Additionally, considering in simulations the blunting of the crack due to the high ductility of the brazing alloy and the resulting plasticity, would have yielded better estimation of J-integrals, potentially decreasing their amplitude. Along the crack blunting, creep and fatigue processes may also impact the stress-strain field (ie. creep stress relaxation and fatigue hardening). Coupled with anisotropy of brazed-joints notably at interfaces, creep and fatigue processes would make the prediction of crack-growth and the estimation of structural integrity lifetime complex. Further 3D simulations, based on experimental work on brazed joints and accounting for such mechanisms will be conducted as further work to better asses the structural integrity of the DEMO FW cooling assemblies.

CONCLUSION

Elastic-plastic simulations were conducted on a reference design of the DEMO first wall cooling channels under a range of steady-state incoming HHF. Simulations reveal significant thermal stresses and strains resulting from thermal expansion mismatch, notably at the interface separating the tungsten tiles to Eurofer97. The estimations of J-integrals around a defect located at the center of the interlayer suggest that crack-growth may first be principally driven by heat fluxes intensities and by crack length solely short defect sizes (a < 500 µm**)**. The comparison of obtained J-integrals with the initiation fracture toughness of copper alloys indicates that some copper alloys may not be able withstand HHF of 1 MW.m^{-2}. With concerns for the structural integrity of brazed-joints in cooling assemblies, further research should investigate ductile/thicker brazed joints and their effect on the first wall structural integrity when sustaining high heat fluxes.

ACKNOWLEDGMENT

Financial support through the EPSRC Centre for Doctoral Training in Nuclear Energy Futures (EP/S023844/1) and the United Kingdom Atomic Energy Authority are gratefully acknowledged. Dr. Yiqiang Wang would like to acknowledge the EPSRC grant EP/T012250/1 and the UK Government Department for Business, Energy and Industrial Strategy (BEIS).

REFERENCES

[1] G. Aiello, J. Aubert, N. Jonqueres, A. Li Puma, A. Morin and G. Rampal, "Development of the Helium Cooled Lithium Lead Blanket for DEMO," *Fusion Engineering and Design,* vol. 89, pp. 1444-1450, 2014.

[2] J. Aubert, G. Aiello, C. Bachmann, P. A. Di Maio, R. Giammusso, A. Li Puma, A. Morin and A. Tincani, "Optimization of the first wall for the DEMO water cooled lithiu; lead blanket," *Fusion Engineering and Design,* Vols. 98-99, pp. 1206-1210, 2015.

[3] G. Federici, W. Biel, M. R. Gilbert, R. Kemp, N. Taylor and R. Wenniger, "European DEMO design strategy and consequences for materials," *Nuclear Fusion,* vol. 57, 2017.

[4] S. Tahtinen, P. M., S. B. and P. Toft, "Tensile and fracture toughness of copper alloys and their HIP joints with austenetic stainless steel in unirradiated and neutron irradiated conditions," CTT manufacturing technology, Roskilde, 1998.

[5] G. Perez, T. Barrett, G. Ellwood, M. Kovari, Z. Vizvary and R. Otin, "A de-coupled DEMo first wall: design concept and preliminary analysis," *Fusion Engineering and design,* 2016.

[6] M. Smith, ABAQUS/Standard user's manual, Verison 6.9, Dassault Systemes Simulia Corp., 2009.

[7] F. Tavassoli, "Fusion DEMO interim Structural Design Criteria (DISDC), Appenndix A: material design limiy data A3.S18E Eurofer steel," CEA, DEN, 2004.

[8] M. A. Meyers, Dynamic behavior of materials, John Wiley & Sons, 1994.

[9] G. Johnson and W. Cook, "A constitutive model and data for metals subjected to large strains, high strain rate sand high temperatures," *Proceedings of the 7th International Symposium on Ballistics,* p. 541–547, 1983.

[10] D. W. Lee, Y. Dug Bae, S. Kwon Kim, B. Guen Hong, H. Kyu Jung, J. Yong Park, Y. Hwan Jeong and N. Kwon Choi, "High heat flux test with HIP bonded BE/Cu/SS mock-ups for the ITER first wall," *Fusion Engineering and Design,* vol. 84, pp. 1160-1163, 2009.

[11] F. C. Nix and D. MacNair, "The thermal expansion of pure metals: copper, gold, aluminum, nickel and iron," *Physical review,* vol. 60.8, p. 597, 1941.

[12] A. P. Miller and A. Cezarliyan, "Thermal expansion of tungsten in the range 1500-3600K by a transient interferometric technique," *International journal of thermophysics,* Vols. 11, No. 4, 1990.

[13] J. G. Hust and A. B. Lankford, "Thermal conductivity of aluminum, copper, iron and tungsten for temperatures from 1K to the melting point," National bureau of standards, U.S. Department of commerce, 1984.

[14] P. Hidnert and W. T. Sweeney, Thermal expansion of tungsten, US givernment printing office, 1925.

[15] J. W. Davis, "ITER material properties handbook," International Atomic Energy Agency, 1994.

[16] T. Chetkov, J. Aktaa and O. Kraft, "Mechanical characterization and modeling ofbrazed EUROFER-tungsten-joints," *Journal of nuclear material,* no. 67–370 , p. 1228–1232, 2007.

[17] D. Bachurina, A. Suchkov, B. Kalin, O. Sevriukov, I. Fedotov, Dzhmaev P., A. Ivannikov, M. Leont'eva-Smirnova and E. Mozhanov, "Joining of tungsten with low-activaion ferritic-martensitic steel and vanadium alloys for DEMO reactor," *Nuclear materials and energy,* vol. 15, pp. 135-142, 2018.

[18] W. Ramberg and W. Osgood, "Description of stress-strain curves by three parameters," Technical note No. 902, National Advisory Committee for aeronautics, Washington DC, 1943.